Outage Probability Analysis of User-Centric SBS based HCNets under Hybrid Rician/Rayleigh Fading

Ziaul Haq Abbas, Arif Ullah, Ghulam Abbas, Fazal Muhammad, and Frank Y. Li

Abstract

To model dense user equipment (UE) distribution in heterogeneous cellular networks (HCNets), the Poisson cluster process (PCP) has emerged as a promising tool. In user-centric HCNets where UEs are distributed according to a PCP around a small base station (SBS), the network performance has been commonly studied in literature under a Rayleigh fading environment assumption. However, such an assumption may not hold in user-centric HCNets given the possible existence of a strong line-of-sight (LOS) link between UEs and BSs due to a relatively short transmission distance. This letter analyzes the performance of user-centric SBS based HCNets by considering that the desired LOS link experiences Rician fading whereas interferer links experience non-LOS Rayleigh fading. Numerical results, validated through extensive simulations, demonstrate that the outage probability decreases under this hybrid Rician/Rayleigh fading environment.

Index Terms

Clustered UEs, heterogeneous cellular network, Rician/Rayleigh fading, user-centric SBS deployment.

I. Introduction

A heterogeneous cellular network (HCNet) comprises of small base stations (SBSs) overlaid by the coverage area of macro base stations (MBSs). In conventional HCNets, the locations of UEs and base stations (BSs) are modeled using independent homogenous Poisson point processes (PPPs) [1] [2]. However, in user-centric HCNets which are considered by the third-generation partnership project (3GPP) as one of the fundamental network topologies for 5G deployment, SBSs are located in hotspots with a high UE density around them. Such a deployment scenario is able to avoid coverage holes and increase network capacity [3]. According to 3GPP, a capacity-driven user-centric SBS network topology is more realistic for 5G deployment in comparison with the conventional PPP based HCNets [4].

To bridge the gap between 3GPP simulation model and the conventional HCNet model, a user-centric approach for SBS deployment was proposed in HCNets [5], where the locations of SBSs and MBSs follow independent homogeneous PPPs, while UEs are assumed to be deployed around SBSs according to a Poisson cluster process (PCP). Different HCNet models, based on clustered stochastic geometry, were analyzed for coverage improvement in [6]. Most existing literature on user-centric SBS deployment assumes a Rayleigh fading link between UEs and BSs for the desired as well as interferer links to ensure analytical tractability [4]–[6]. The performance of user-centric SBS deployment was investigated in millimeter-wave HCNet in [7], while considering Nakagami-m fading for both line-of-sight (LOS) and non-line-of-sight (NLOS) signals. In the user-centric SBS based HCNets, the UEs are located closer to a BS. Therefore, it is more probable that there is a LOS component between the UEs and the serving BS. Due to short transmission distance, Rician fading is more appropriate for an LOS transmission link [8]. Compared to a serving BS, the interferer BSs are located farther from a UE. This leads to the assumption that interferer BSs are NLOS and experience Rayleigh fading.

The performance of conventional HCNets in Rician fading and device-to-device communication overlaid by HCNets in generalized fading was studied in [9] and [10], respectively. The authors in [11] analyzed HCNets by assuming a Rician/Rayleigh fading environment. The authors in [9]–[11] considered uniformly distributed UEs and BSs throughout the network. Contrarily, this letter investigates the communication failure probability (outage probability) metric, by considering user-centric SBS deployment in HCNets under a hybrid Rayleigh/Rician fading environment. More specifically, this letter assumes that the desired received signal experiences Rician fading while the interferer signal experiences Rayleigh fading in the user-centric SBS based HCNets. The main contribution of this paper is that we analyze the performance of user-centric SBS deployed HCNets in a hybrid Rician/Rayleigh fading environment. Furthermore, we also separately characterize the performance of a cluster serving SBS. Numerical results demonstrate that the performance of cluster serving SBS and BSs in other tiers are improved in such fading environment thanks to the existence of strong LOS between UE and SBS.

II. System Model and Fading Assumptions

As opposed to the conventional HCNet model with uniformly distributed UEs and BSs via PPP distributions, a user-centric model assumes clustered UEs around SBS. Hence, UEs and BSs follow two different distributions.

Z. H. Abbas, A. Ullah, and G. Abbas are with the TeleCoN Research Lab, GIK Institute of Engineering Sciences and Tecnology, Topi, 23460, Pakistan. E-mail: {ziaul.h.abbas, arifullah, abbasg}@giki.edu.pk.

F. Muhammad is with the City University of Science and Information Technology Peshawar, 25000, Pakistan. E-mail: fazal.muhammad@cusit.edu.pk.

F. Y. Li is with the University of Agder, N-4898, Grimstad, Norway. E-mail: frank.li@uia.no.

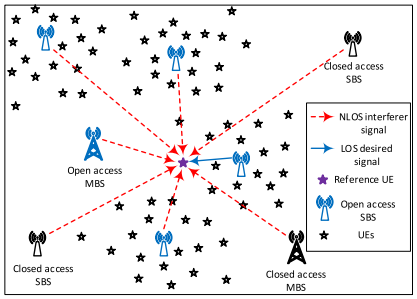

Fig. 1: Two-tier HCNet with user-centric SBS deployment.

A. Network Layout

We consider a multi-tier HCNet model with downlink transmission, where SBSs are positioned in the areas with high UE density as shown in Fig. 1. We assume that the ith tier of BSs consists of open access (oa) and closed access (ca) BSs, distributed via homogeneous PPPs, Φ_i^{oa} and Φ_i^{ca}, with deployment densities λ_i^{oa} and λ_i^{ca}, respectively. Open access BSs are those to which UEs can associate, whereas closed access BSs are licensed and only act as interferers for the reference UE (a randomly selected UE from a cluster). The ith tier BSs are distinguished from each other by transmit power P_i and association bias B_i, however, $P_i^{\text{oa}} = P_i^{\text{ca}}$ and $B_i^{\text{oa}} = B_i^{\text{ca}}$. The path loss exponent of the ith tier transmitted signal is $\alpha_i > 2$. In user-centric SBS deployment, the SBSs are located at the center of each UE cluster. Hereafter, we assume that UEs are distributed according to two special cases of a PCP, i.e., Thomas cluster process (TCP) and Matern cluster process (MCP). In TCP, clustered UEs are distributed around an SBS according to Gaussian distribution with variance σ, whereas in case of MCP the clustered UEs are uniformly distributed around an SBS in a circular a disc with radius R. The UE density across the network is $\lambda_u^{\text{pcp}} = N_c \lambda_i^{\text{oa}}$, where N_c denotes the number of UEs per cluster. The value of σ shows the deviation of clustered UEs' random distances from the SBS located at the center of each cluster. The number of tiers, $\mathcal{M}$, is enriched with the 0th tier, consisting of a single cluster serving SBS located at the cluster center, and the second tier ($i = 2$) comprising of a number of SBSs located outside the randomly selected cluster, such that $\mathcal{M} = 0 \cup \mathcal{B}$ where $\mathcal{B} = \{1, 2, ...\}$.

Our analysis is performed based on a randomly selected UE, also termed as a reference UE, from an arbitrarily selected cluster, called a representative cluster. Without loss of generality, we assume that the reference UE is located at the origin and follows the maximum biased received power (BRP) association strategy. The location of the nearest BS belonging to ith tier, x_i^* $\forall i \in \mathcal{M}$, is given by

$$x_i^* = \arg \max_{x_i \in \Phi_i^{\text{oa}}} P_i B_i x_i^{-\alpha_i}, \tag{1}$$

where B_i and x_i are association bias and distance of the ith tier BSs, respectively. The instantaneous received power by the reference UE is $P_r = P_i G x_i^{-\alpha_i}$, where G denotes fading gain.

B. Fading Environment

We assume a Rician/Rayleigh fading environment wherein the NLOS interfering signals follow Rayleigh fading and the LOS desired signal experiences Rician fading. When the received link is LOS, G follows non-central chi-squared distribution with unit mean. The probability density function (PDF) of G, $f_G(g)$, is given by [11]

$$f_G(g) = (1+K)\exp(-K-(1+K)g) I_0\left(2\sqrt{K(1+K)g}\right), \tag{2}$$

where I_0 is a modified Bessel function and K is the Rician factor with a value ranging between 1 and 10. Using the exponential series approximation, the PDF in (2) can be rewritten as

$$f_G(g) \approx \sum_{n=1}^{N} \chi_n \mu_n \exp(-\mu_n g), g \in [0, X], \tag{3}$$

where N is the total number of terms in the exponential series, and χ_n and μ_n are real valued numbers, such that $\mu_n > 0$. X is the limit of the summation in (5). The value of N is set to achieve a desired level of accuracy. The average complementary cumulative distribution function (CCDF) of the desired received signal power can be obtained by integrating (3) as

$$\overline{E}_G(g) = \sum_{n=1}^{N} \chi_n \exp(-\mu_n g), g \in [0, X]. \tag{4}$$

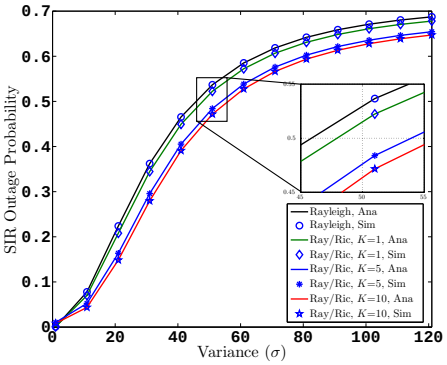

Fig. 2: Total outage probability versus variance for TCP.

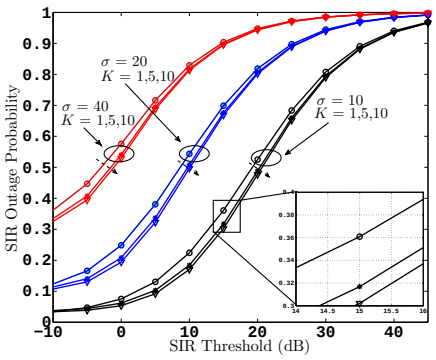

Fig. 3: Cluster center SBS outage probability versus SIR threshold for TCP.

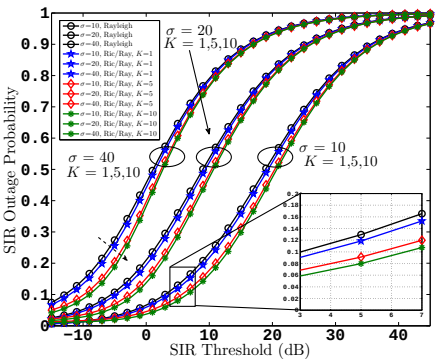

Fig. 4: Total outage probability versus SIR threshold for TCP.

The coefficients χ_n and μ_n are determined by solving a non-linear optimization problem, formulated as

$$\begin{aligned} \min_{\chi_n,\mu_n} \quad & \int_0^X \left(\overline{E}_G(g) - \overline{F}_G(g)\right)^2 dg \\ \text{s.t.,} \quad & \sum_{n=1}^{X} \chi_n = 1, \\ & \mu_n > 0 \qquad\qquad \forall n \in \{1,2,...,N\}. \end{aligned} \tag{5}$$

The optimization problem is solved in polynomial time using the interior point method. $\overline{F}_G(g)$ denotes the CCDF of G and is obtained from (2). The initial value of χ_n and μ_n are selected from the standard normal distribution. The estimated values of χ_n and μ_n are given in Table I.

To avoid notational complexity, we define

$$\hat{P}_j = (P_j/P_i)^{1/\alpha_j}, \hat{B}_j = (B_j/B_i)^{1/\alpha_j}, \hat{\alpha}_j = \alpha_j/\alpha_i, \tag{6}$$

where $P_j(P_i)$, $B_j(B_i)$ and $\alpha_j(\alpha_i)$ are the transmit power, association bias, and path loss exponent of jth tier interfering (ith tier serving) BSs, respectively.

III. Association probability and distribution of serving distances

In this section, we derive the association probability and distance distribution of a reference UE with the serving BS. The serving BS is the nearest BS from PPP distribution Φ_i^{oa}, located at y_i. The distributions of random variable y_i are given as

$$\text{PDF:} \quad f_{Y_i}(y_i) = 2\pi\lambda_i^{\text{oa}} y_i \exp\left(-\pi\lambda_i^{\text{oa}} y_i^2\right), y_i \geq 0, \tag{7a}$$

$$\text{CCDF:} \quad F_{Y_i}(y_i) = \exp\left(-\pi\lambda_i^{\text{oa}} y_i^2\right), \qquad y_i \geq 0. \tag{7b}$$

Considering that the reference UE is located at the origin and is y_0 distance away from the cluster center SBS, the distributions of y_0 in case of TCP are given as

$$\text{PDF:} \quad f_{Y_0}(y_0) = y_0/\sigma^2 \exp\left(-y_0^2/2\sigma^2\right), y_0 \geq 0, \tag{8a}$$

$$\text{CCDF:} \quad F_{Y_0}(y_0) = \exp\left(-y_0^2/2\sigma^2\right), \qquad y_0 \geq 0. \tag{8b}$$

Similarly, the distributions of y_0 for MCP are given as

$$\text{PDF:} \quad f_{Y_0}(y_0) = 2y_0/R^2, \qquad y_0 \leq R, \tag{9a}$$

$$\text{CCDF:} \quad F_{Y_0}(y_0) = (R^2 - y_0)/R^2, y_0 \leq R. \tag{9b}$$

The association probability, $\mathcal{A}_i$, and the PDF, $f_{Y_i}^{\text{pcp}}(y_i)$, of serving distances are defined, respectively, as

TABLE I: Coefficients χ_n and μ_n for selected values of K and N

N	$K=1$		$K=5$		$K=10$	
	χ_n	μ_n	χ_n	μ_n	χ_n	μ_n
$n=1$	-0.8993	1.2475	42.279	2.9576	177.750	3.8741
$n=2$	5.9324	1.4298	-189.999	3.7559	-338.049	4.3761
$n=3$	-5.4477	1.7436	192.999	4.1436	297.000	5.3985
$n=4$	1.4145	1.4145	-44.289	4.7715	-44.289	5.9937

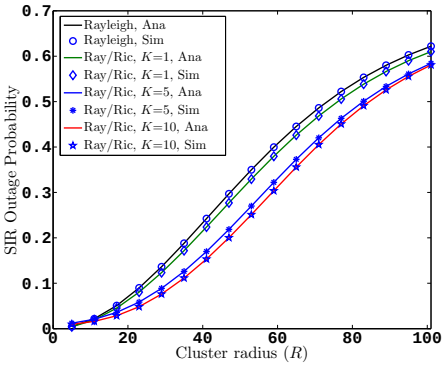

Fig. 5: Total outage probability versus cluster radius for MCP.

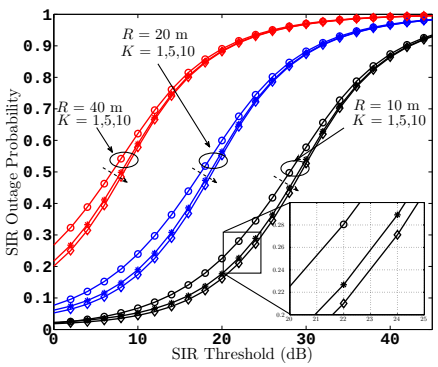

Fig. 6: Cluster center SBS outage probability versus SIR threshold for MCP.

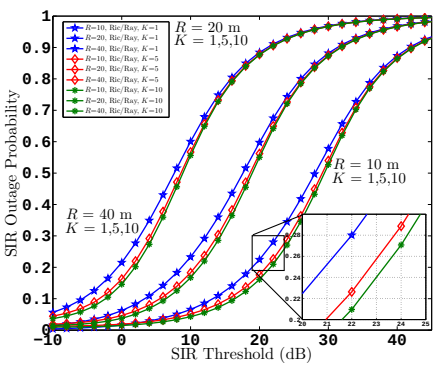

Fig. 7: Total outage probability versus SIR threshold for MCP.

$$\mathcal{A}_i = \begin{cases} \int_0^\infty \exp\left\{ -\pi \sum_{\substack{j\in\mathcal{M}\\ j\neq i}} \lambda_i^{\text{oa}} \hat{B}_j \hat{P}_j^2 y_0^2 \right\} f_{Y_0}(y_0) dy_0, & \text{if } i = 0, \\ \int_0^\infty \exp\left\{ -\pi \sum_{\substack{j\in\mathcal{M}\\ j\neq i}} \lambda_i^{\text{oa}} \hat{B}_j \hat{P}_j^2 y_i^2 \right\} F_{Y_0}(\hat{B}_j \hat{P}_j^2 y_j) f_{Y_i}(y_i) dy_i, & \\ & \text{if } i \in \mathcal{B}. \end{cases} \tag{10}$$

Proof. See Appendix A. ■

$$f_{Y_i}^{\text{pcp}}(y_i) = \begin{cases} \frac{1}{\mathcal{A}_0} \exp\left\{ -\pi \sum_{\substack{j\in\mathcal{M}\\ j\neq i}} \lambda_i^{oa} \hat{B}_j \hat{P}_j^2 y_0^2 \right\} f_{Y_0}(y_0), & \text{if } i = 0, \\ \frac{1}{\mathcal{A}_i} \exp\left\{ -\pi \sum_{\substack{j\in\mathcal{M}\\ j\neq i}} \lambda_i^{oa} \hat{B}_j \hat{P}_j^2 y_i^2 \right\} F_{Y_0}(\hat{B}_j \hat{P}_j^2 y_j) f_{Y_i}(y_i), & \\ & \text{if } i \in \mathcal{B}. \end{cases} \tag{11}$$

Proof. See Appendix B. ■

The PDF and CCDF of Y_i in (10) and (11) are given in (7), while the PDF and CCDF of Y_0 in case of TCP and MCP are given in (8) and (9), respectively.

IV. Outage Probability

In this section, we evaluate the outage probability of user-centric SBS deployed HCNets under a Rican/Rayleigh fading environment. Outage probability is defined as the probability that the signal-to-interference ratio (SIR) level received by the reference UE, which is associated with an ith tier BS, is lower than the predefined SIR threshold Ω. The total outage probability can be defined as

$$\mathbb{O}_t^{\text{pcp}} = \mathcal{A}_0 \mathbb{O}_0^{\text{pcp}} + \mathcal{A}_i \mathbb{O}_i^{\text{pcp}}, \tag{12}$$

where per tier outage probability $\mathbb{O}_0^{\text{pcp}}$ and $\mathbb{O}_i^{\text{pcp}}$ are defined in Theorem 1.

Theorem 1. The per tier outage probability of a reference UE from clustered UE set in the proposed system model, given that the UE is associated with ith tier open access BS, is given as (13), where $\mathbb{Z}(\mu_n \Omega_i, \alpha_i, \hat{B}_j) = \frac{2\mu_n \Omega_i B_i^{2/\alpha_i - 1}}{\alpha_i - 2} {}_2F_1\left[1, 1 - \frac{2}{\alpha_i}; 2 - \frac{2}{\alpha_i}; -\frac{\mu_n \Omega_i}{\hat{B}_j}\right]$, σ is the variance of UE locations, and $\mathbb{Q}(\mu_n \Omega_i, \alpha_i) = \mu_n \Omega_i^{2/\alpha_i} \frac{2\csc(\frac{2\pi}{\alpha_i})}{\alpha_i}$. Here, ${}_2F_1[.]$ is the Hyper-geometric function and $\mathcal{L}_{\mathcal{I}_{(i,0)}^{\text{oa}}}(.)$ denotes the Laplace transform of interference from the cluster center SBS. $f_{Y_0}^{\text{pcp}}(y_0)$ and $f_{Y_i}^{\text{pcp}}(y_i)$ are given in (11).

Proof. See Appendix C. ■

$$\mathbb{O}_i^{\text{pcp}} = \begin{cases} 1 - \int\limits_0^{\infty} \sum\limits_{n=1}^{N} \chi_n \exp\Big\{ -\pi \sum\limits_{\substack{j\in\mathcal{M}\\ j\neq i}} \hat{P}_j^{2/\alpha_i} \Big(\lambda_j^{\text{oa}} \big[\hat{B}_j + \mathbb{Z}(\mu_n\Omega_i, \alpha_i, \hat{B}_j)\big] + \lambda_j^{\text{ca}} \mathbb{Q}(\mu_n\Omega_i, \alpha_i) \Big) y_0^2 \Big\} f_{Y_0}^{\text{pcp}}(y_0) dy_0, & \text{if } i = 0, \\ 1 - \int\limits_0^{\infty} \sum\limits_{n=1}^{N} \chi_n \exp\Big\{ -\pi \sum\limits_{\substack{j\in\mathcal{M}\\ j\neq i}} \hat{P}_j^{2/\alpha_i} \Big(\lambda_j^{\text{oa}} \big[\hat{B}_j + \mathbb{Z}(\mu_n\Omega_i, \alpha_i, \hat{B}_j)\big] + \lambda_j^{\text{ca}} \mathbb{Q}\big(\mu_n\Omega_i, \alpha_i\big) \Big) y_i^2 \Big\} \mathcal{L}_{(i,0)}^{oa}\Big(\frac{\Omega_i y_i^{\alpha_i}}{P_i} \Big) f_{Y_i}^{\text{pcp}}(y_i) dy_i, & \\ & \text{if } i \in \mathcal{B}. \end{cases} \tag{13}$$

V. Numerical Results

In this section, we discuss the impact of Rician/Rayleigh fading on outage probability in user-centric SBS based HCNets. For the sake of illustration clarity, we consider a two-tier HCNet model for simulations which consist of an MBS tier with density $\lambda_1^{\text{oa}} = 1/(\pi 1000^2)$ and transmit power $P_1 = 53$ dBm, and an SBS tier with density $\lambda_2^{\text{oa}} = 100\lambda_1^{\text{oa}}$ and transmit power $P_2 = 33$ dBm. The association bias $B_1 = B_2 = 0$ dB and $\alpha_1 = \alpha_2 = 3.5$. We consider $N = 4$ number of terms in the exponential series.

In Fig. 2, the total SIR outage probability for different values of σ in case of TCP is plotted. Similarly, for MCP the total SIR outage probability versus R for different values of K is plotted in Fig. 5. The outage probability increases as cluster parameters (σ for TCP and R for MCP) increase because the cluster size becomes larger for higher values of σ and R. In a large cluster, UEs are located farther from the cluster center SBS. In Figs. 2 and 5, it can be observed that the analytical results closely fit the simulation results and the outage probability decreases when K increases from 1 to 10. Even for $K = 1$, the performance of Rician/Rayleigh is better than the Rayleigh-fading-only case because of the existence of an LOS link.

In Figs. 3 and 6, we plot the outage probability of the cluster center SBS for TCP and MCP, respectively. The outage probability of cluster center SBS decreases when K increases from 1 to 10. For a lower range of the SIR threshold, considerable improvement in outage probability is observed because the effect of severe fading is weaker for a constant LOS component.

In Figs. 4 and 7, the total outage probability versus the SIR threshold for TCP and MCP, respectively, is presented. The total outage probability is higher for larger values of σ and R in case of TCP and MCP, respectively. This is because the UEs are located closer to SBSs for a smaller value of σ and R. Fig. 4 demonstrates that for 10% of outage performance, the SIR threshold decreases from 7 dB to 3 dB for $K = 5$. Furthermore, Figs. 4 and 7 demonstrate that for $\sigma = 10$ and $R = 10$ m, a significant performance gain is observed for a lower range of SIR threshold in hybrid Rician/Rayleigh fading environment. Again this benefit is obtained owing to the significant fading reduction when a direct LOS signal exists.

VI. Conclusion

This paper analyzes the outage probability of user-centric SBS deployment in HCNets based on a hybrid Rician/Rayleigh fading assumption. The outage probability is derived by modeling the dominant LOS signal using finite exponential-series approximation of non-centeral chi square distribution. Simulation results validate the proposed model. We find that the outage probability of cluster serving SBS decreases for higher Rician factor due to the existence of a strong LOS component. It is concluded that the performance of HCNets with user-centric SBS deployment is improved in a hybrid Rician/Rayleigh fading environment.

Appendix

A. Proof of (10)

The association probability of a cluster center SBS, i.e., $i = 0$, can be expressed as

$$\mathcal{A}_0 = \mathbb{E}_{Y_0}\Big\{ \prod_{\substack{j\in\mathcal{M}\\ j\neq i}} \mathbb{P}\big(Y_0 > \hat{B}_j \hat{P}_j Y_j\big) \Big\} = \int_0^{\infty} \prod_{\substack{j\in\mathcal{M}\\ j\neq i}} F_{Y_i}\big(\hat{B}_j \hat{P}_j Y_j\big) f_{Y_0}(y_0) dy_0.$$

The association probability of BSs located outside clusters, i.e., $i \in \mathcal{B}$, can be obtained as

$$\mathcal{A}_i = \mathbb{E}_{Y_i}\Big\{ \prod_{\substack{j\in\mathcal{M}\\ j\neq i}} \mathbb{P}\big(Y_i > \hat{B}_j \hat{P}_j Y_j\big) \Big\} = \int_0^{\infty} F_{Y_0}\big(\hat{B}_j \hat{P}_j Y_j\big) \prod_{\substack{j\in\mathcal{M}\\ j\neq i}} F_{Y_i}\big(\hat{B}_j \hat{P}_j X_j\big) f_{Y_i}(y_i) dy_i.$$

The PDF and CCDF of Y_0 for TCP and MCP are given in (8) and (9), respectively. Similarly, the PDF and CCDF of Y_i are given in (7).

B. Proof of (11)

The PDF of serving distances for $i=0$, is given by

$$f_{Y_0}^{\text{pcp}}(y_0)=\frac{d}{dy}\mathbb{P}\Big\{Y_0>y|\mathcal{A}_0\Big\}=\frac{d}{dy}\Big\{\frac{\mathbb{P}\big(Y_0>\hat{B}_j\hat{P}_jY_j\big)}{\mathcal{A}_0}\Big\}$$

$$=\frac{1}{\mathcal{A}_0}\frac{d}{dy}\Big\{\int_x^{\infty}\prod_{\substack{j\in\mathcal{M}\\ j\neq i}}F_{Y_i}\big(\hat{B}_j\hat{P}_jY_j\big)f_{Y_0}(y_0)dy_0\Big\}$$

$$=\frac{1}{\mathcal{A}_0}\prod_{\substack{j\in\mathcal{M}\\ j\neq i}}F_{Y_i}\big(\hat{B}_j\hat{P}_jX_j\big)f_{Y_0}(y_0). \tag{14}$$

Similarly, the PDF of serving distances from BSs located outside the cluster, i.e., $i\in\mathcal{B}$, can be obtained as

$$f_{Y_i}^{\text{pcp}}(y_i)=\frac{1}{\mathcal{A}_i}F_{Y_0}\big(\hat{B}_j\hat{P}_jY_j\big)\prod_{\substack{j\in\mathcal{M}\\ j\neq i}}F_{Y_i}\big(\hat{B}_j\hat{P}_jY_j\big)f_{Y_i}(y_i). \tag{15}$$

C. Proof of Theorem 1

The outage probability of clustered UEs is written as

$$\mathbb{O}_i^{\text{pcp}}=1-\int_0^{\infty}\Big\{P\Big(\text{SIR}\big(y_i\big)>\Omega_i\Big)\Big\}f_{Y_i}^{\text{pcp}}(y_i)dy_i, \tag{16}$$

where $\mathbb{P}\big(\text{SIR}(y_i)>\Omega_i\big)$

$$=\mathbb{P}\Big(g_i>\frac{\Omega_i y_i^{\alpha_i}}{P_i}\Big(\sum_{\substack{i\in\mathcal{M}\\ j\in\Phi_i}}\mathcal{I}_{(i,j)}^{\text{oa}}+\sum_{\substack{i\in\mathcal{M}\\ j\in\Phi_i}}\mathcal{I}_{(i,j)}^{\text{ca}}\Big)\Big)$$

$$\overset{\text{(a)}}{=}\prod_{\substack{j\in\mathcal{M}\\ j\in\Phi_i}}\mathcal{L}_{\mathcal{I}_{(i,j)}^{\text{oa}}}\Big(\frac{\Omega_i y_i^{\alpha_i}}{P_i}\Big)\prod_{\substack{j\in\mathcal{M}\\ j\in\Phi_i}}\mathcal{L}_{\mathcal{I}_{(i,j)}^{\text{ca}}}\Big(\frac{\Omega_i y_i^{\alpha_i}}{P_i}\Big),$$

$$\overset{\text{(b)}}{=}\sum_{n=1}^{X}\chi_n\prod_{\substack{j\in\mathcal{M}\\ j\in\Phi_i}}\mathcal{L}_{\mathcal{I}_{(i,j)}^{\text{oa}}}\Big(\frac{\mu_n\Omega_i y_i^{\alpha_i}}{P_i}\Big)\prod_{\substack{j\in\mathcal{M}\\ j\in\Phi_i}}\mathcal{L}_{\mathcal{I}_{(i,j)}^{\text{ca}}}\Big(\frac{\mu_n\Omega_i y_i^{\alpha_i}}{P_i}\Big). \tag{17}$$

In (17), Step (a) is due to the independence of processes Φ_i^{oa} and Φ_i^{ca}. Step (b) follow exponential series approximation in (4). Using (16) and (17), the outage probability, given that the UE connects to *i*th tier BS, is given by (18) and (19).

For the 0th tier, i.e., $(i=0)$: The outage probability, given that when the UE connects to the cluster center SBS, can be written as

$$\mathbb{O}_0^{\text{pcp}}=1-\int_0^{\infty}\sum_{n=1}^{X}\chi_n\prod_{\substack{j\in\mathcal{M}\\ j\in\Phi_i}}\mathcal{L}_{\mathcal{I}_{(i,j)}^{\text{oa}}}\Big(\frac{\mu_n\Omega_i y_i^{\alpha_i}}{P_i}\Big)$$
$$\times\prod_{\substack{j\in\mathcal{M}\\ j\in\Phi_i}}\mathcal{L}_{\mathcal{I}_{(i,j)}^{\text{ca}}}\Big(\frac{\mu_n\Omega_i y_i^{\alpha_i}}{P_i}\Big)f_{Y_0}^{\text{pcp}}(y_0)dy_0. \tag{18}$$

For the *i*th tier where $i\in\mathcal{B}$ and $i\neq 0$: Similarly, the per tier outage probability, when the UE connects to a BS, other than the cluster center SBS, can be expressed as

$$\mathbb{O}_i^{\text{pcp}}=1-\int_0^{\infty}\sum_{n=1}^{X}\chi_n\prod_{\substack{j\in\mathcal{M}\\ j\in\Phi_i}}\mathcal{L}_{(i,j)}^{\text{oa}}\Big(\frac{\Omega_i y_i^{\alpha_i}}{P_i}\Big)\mathcal{L}_{\mathcal{I}_{(i,0)}^{\text{oa}}}\Big(\frac{\mu_n\Omega_i y_i^{\alpha_i}}{P_i}\Big)$$
$$\times\prod_{\substack{j\in\mathcal{M}\\ j\in\Phi_i}}\mathcal{L}_{\mathcal{I}_{(i,j)}^{\text{ca}}}\Big(\frac{\mu_n\Omega_i y_i^{\alpha_i}}{P_i}\Big)f_{Y_i}^{\text{pcp}}(y_i)dy_i. \tag{19}$$

Here, $\mathcal{L}_{\mathcal{I}^{\text{oa}}_{(i,0)}}(.)$ is the Laplace transform of interference from the cluster center SBS ($\mathcal{I}^{\text{oa}}_{(i,0)}$). $\mathcal{L}_{\mathcal{I}^{\text{oa}}_{(i,j)}}(.)$ and $\mathcal{L}_{\mathcal{I}^{\text{ca}}_{(i,j)}}(.)$ represent the Laplace transforms of interferences from open access BSs $\mathcal{I}^{\text{oa}}_{(i,j)}$ and closed access BSs $\mathcal{I}^{\text{oa}}_{(i,j)}$, located outside representative cluster, given as (20) and (21), respectively.

$$\mathcal{L}_{\mathcal{I}^{\text{oa}}_{(i,j)}}\left(\frac{\Omega_i y_i^{\alpha_i}}{P_i}\right) = \mathbb{E}_{\mathcal{I}^{\text{oa}}_{(i,j)}}\left[\exp\left\{-\frac{\mu_n \Omega_i y_i^{\alpha_i} \mathcal{I}^{oa}_{(i,j)}}{P_i}\right\}\right]$$

$$= \exp\left\{-\pi\lambda_i^{\text{oa}} \hat{P}_j^{\,2} \mathbb{Z}(\mu_n\Omega_i, \alpha_i, \mathcal{B}_i) y_i^2\right\}. \tag{20}$$

Furthermore, the Laplace transform of interference from closed access BSs is independent of y_i. Thus, it can simply be obtained by making the lower limit of integral equal to zero in the case of open access, and it is given as

$$\mathcal{L}_{\mathcal{I}^{\text{ca}}_{(i,j)}}\left(\frac{\Omega_i y_i^{\alpha_i}}{P_i}\right) = \exp\left\{-\pi\lambda_i^{\text{ca}} \mathbb{Q}(\mu_n\Omega_i, \alpha_i) \hat{P}_j^{2/\alpha_i} y_i^2\right\}. \tag{21}$$

$\mathcal{I}^{oa}_{(i,0)}(.)$ in (19) is the interference contributed by the BS located at the center of the representative cluster and its Laplace transform is given by

$\mathcal{L}_{\mathcal{I}^{\text{oa}}_{(i,0)}}\left(\frac{\Omega_i y_i^{\alpha_i}}{P_i}\right)$

$$= \int_{ll}^{\infty} \frac{1}{1 + \frac{\Omega_i y_i^{\alpha_i}}{\hat{B}_i \hat{P}_i} y_0^{-\alpha_i}} f_{Y_0}\left(y_0 | Y_0 > \hat{B}_j \hat{P}_j^{1/\alpha_i} y_i\right) d_{y_0}, \tag{22}$$

where $ll = \hat{B}\hat{P}x_i^{-\alpha_i}$. Substituting (20), (21) and (22) into (18) and (19), completes the proof of Theorem 1.

REFERENCES

[1] F. Muhammad, Z. H. Abbas, and F. Y. Li, "Cell association with load balancing in nonuniform heterogeneous cellular networks: Coverage probability and rate analysis," *IEEE Trans. Veh. Technol.,* vol. 66, no. 6, pp. 5241-5255, Jun. 2017.

[2] M.O. Al-Kadri, Y. Deng, and A. Nallanathan, "Outage probability of heterogeneous cellular networks with full-duplex small cells," in *Proc. IEEE GLOBECOM,* Washington, DC, USA, Dec. 2016.

[3] A. Jaziri, R. Nasri, and T. Chahed, "System level analysis of heterogeneous networks under imperfect traffic hotspot localization," *IEEE Trans. Veh. Technol.*, vol. 65, no. 12, pp. 9862–9872, Dec. 2016.

[4] 3GPP TR 36.872, "Small cell enhancements for E-UTRA and EUTRAN - Physical layer aspects," v.12.1.0, Dec. 2013.

[5] C. Saha, M. Afshang, and H. S. Dhillon, "Enriched K-tier HetNet model to enable the analysis of user-centric small cell deployments," *IEEE Trans. Wireless Commun.*, vol. 16, no. 3, pp. 1593-1608, Mar. 2017.

[6] ——, "3GPP-inspired HetNet model using Poisson cluster process: Sum-product functionals and downlink coverage," *IEEE Trans. Commun.*, vol. 66, no. 5, pp. 2219-2234, May 2018.

[7] X. Wang, E. Turgut, and M. C. Gursoy, "Coverage in downlink heterogeneous mmWave cellular networks with user-centric small cell deployment," *IEEE Trans. Veh. Technol.*, vol. 68, no. 4, pp. 3513-3533, Jan. 2019.

[8] J. K. N. Nyarko and C. A. Mbom, "Performance study of massive MIMO heterogeneous networks with Rician/Rayleigh fading," *Electronics*, vol. 7, no. 6, pp. 2079-9292, May 2018.

[9] B. Blaszczyszyn and H. P. Keeler, "Equivalence and comparison of heterogeneous cellular networks," in *Proc. IEEE PIMRC,* London, U.K., pp. 153–157, Sep. 2013.

[10] Y. J. Chun, S. L. Cotton, H. S. Dhillon, A. Ghrayeb, and M. O. Hasna, "A stochastic geometric analysis of device-to-device communications operating over generalized fading channels," *IEEE Trans. Wireless Commun.*, vol. 16, no. 7, pp. 4151-4165, Jul. 2017.

[11] X. Yang and A. O. Fapojuwo, "Coverage probability analysis of heterogeneous cellular networks in Rician/Rayleigh fading environments," *IEEE Commun. Lett.*, vol. 19, no. 7, pp. 1197-1200, Jul. 2015.